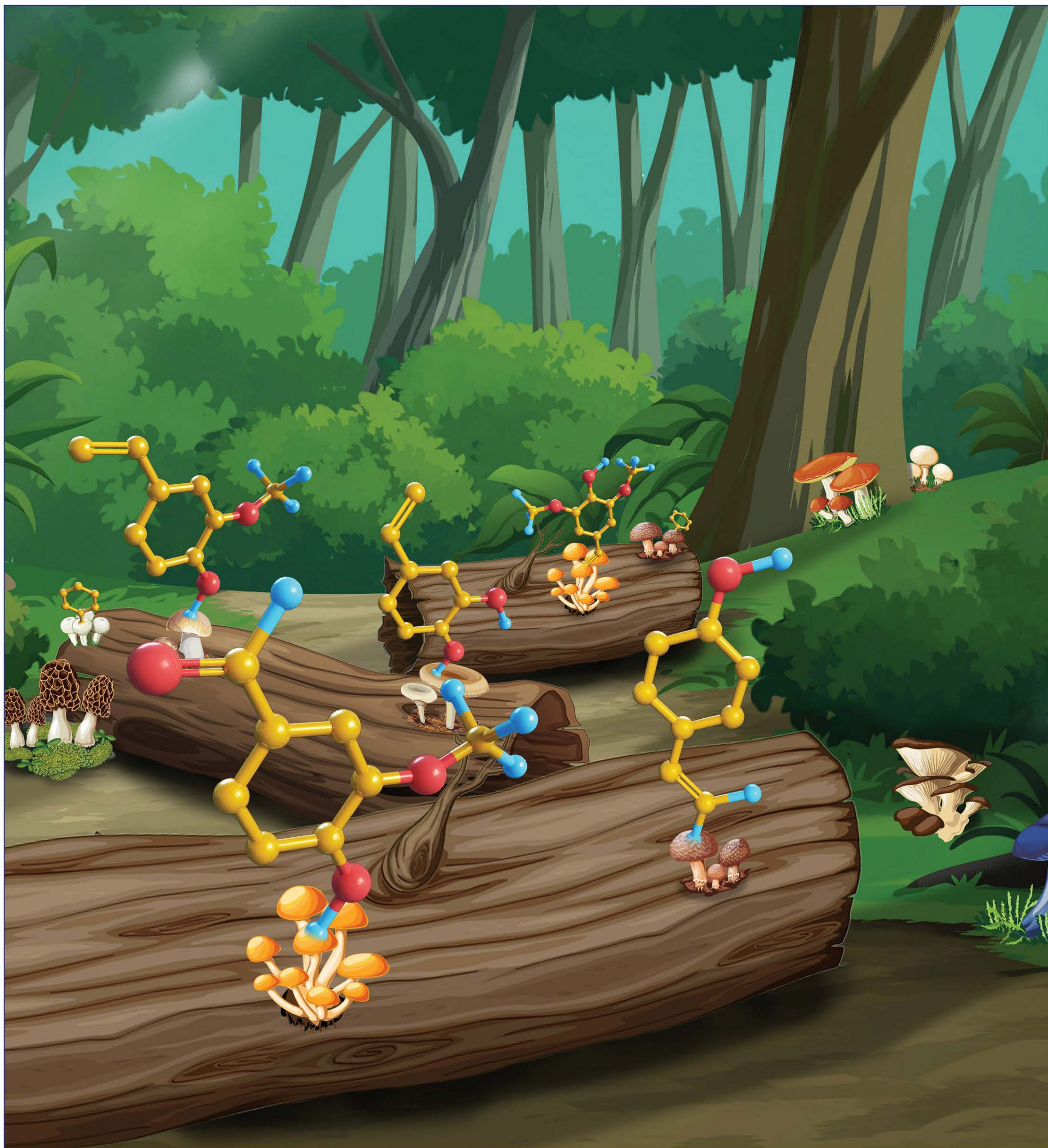


November 28, 2018  
Volume 140  
Number 47  
pubs.acs.org/JACS

# J | A | C | S

JOURNAL OF THE AMERICAN CHEMICAL SOCIETY



ACS Publications  
Most Trusted. Most Cited. Most Read.

[www.acs.org](http://www.acs.org)

**November 28, 2018**

Volume 140, Issue 47

Pages 15985-16368

### About the Cover:

By using two newly identified enzymes with high activities and thermal stabilities, a coenzyme-free biocatalyst was constructed for value-added utilization of lignin hydrolytic aromatics. This green route paves the way for enhancing the entire efficiency of biorefineries.

[View the article.](#)

### In this issue:

- » SPOTLIGHTS
- » PERSPECTIVES
- » COMMUNICATIONS
- » ARTICLES
- » ADDITIONS AND CORRECTIONS
- » MASTHEADS

[Download Hi-Res Cover](#)



**ACS AuthorChoice**   
More about this program



**ACS Editors' Choice**   
More about this program

# A Coenzyme-Free Biocatalyst for the Value-Added Utilization of Lignin-Derived Aromatics

Jun Ni, Yu-Tong Wu, Fei Tao, Yuan Peng, and Ping Xu\*<sup>✉</sup>

State Key Laboratory of Microbial Metabolism, Joint International Research Laboratory of Metabolic & Developmental Sciences, and School of Life Sciences & Biotechnology, Shanghai Jiao Tong University, Shanghai 200240, People's Republic of China

## Supporting Information

**ABSTRACT:** Value-added utilization of lignin waste streams is vital to fully sustainable and economically viable biorefineries. However, deriving substantial value from its main constituents is seriously hindered by the constant requirement for expensive coenzymes. Herein, we devised a coenzyme-free biocatalyst that could transform lignin-derived aromatics into various attractive pharmaceutical and polymer building blocks. At the center of our strategy is the integrated use of new mining phenolic acid decarboxylase and aromatic dioxygenase with extremely high catalytic efficiency, which realizes the value-added utilization of lignin in a coenzyme-independent manner. Notably, a new temperature/pH-directed strategy was proposed to eliminate the highly redundant activities of endogenous alcohol dehydrogenases. The major components of lignin were simultaneously converted to vanillin and 4-vinylphenol. Since the versatile biocatalyst could efficiently convert many other renewable lignin-related aromatics to valuable chemicals, this green route paves the way for enhancing the entire efficiency of biorefineries.

Biorefining of lignocellulosic biomass/agricultural wastes offers a promising route to couple petrochemical replacement with environmental sustainability.<sup>1–3</sup> Conventional biorefineries, together with the pulp and paper industry, generate more than 300 million tons of lignin waste streams annually. The bulk of the lignin is simply burned for heat.<sup>4,5</sup> Recently, catalytic valorization of this largely unexploited resource for renewable chemicals has attracted extensive attention.<sup>6–8</sup> Ferulic acid (**1**) and *p*-coumaric acid (**2**) represent the most predominant aromatic monomers in lignin, which can be efficiently released by thermochemical depolymerization or enzymatic hydrolysis.<sup>6,9</sup> Thus, the development of green processes for converting these accessible lignin-related phenolic acids to value-added products is the key to ensuring more sustainable and competitive biorefineries.<sup>10,11</sup> **1** is one of the practical starting materials for vanillin (**3**), which is a widely used flavor compound and is a building block of thermosetting resins/thermoplastics.<sup>12,13</sup> Feruloyl-CoA synthetase (Fcs) and enoyl-CoA hydratase/aldolase (Ech) are typically responsible for the bioconversion of **1** to **3**.<sup>14</sup> Nevertheless, the constant requirement for ATP and CoA in this biosynthetic route has seriously hindered the effective utilization of **1** and other lignin-derived aromatics.<sup>15,16</sup> To

date, no coenzyme-free biocatalytic process has managed to achieve value-added utilization of lignin hydrolytic aromatics.

To efficiently derive substantial value from the main constituents of lignin in a coenzyme-independent manner, we devised a coenzyme-free biocatalyst containing a phenolic acid decarboxylase (Pad) and aromatic dioxygenase (Ado). The Pad catalyzes the nonoxidative decarboxylation of **1** and **2**, resulting in the formation of 4-vinylguaiacol (**4**) and 4-vinylphenol (**5**), respectively.<sup>17,18</sup> **5** is widely used for polymeric materials, photoresistors, and semiconductor manufacturing.<sup>19,20</sup> Next, an undiscovered enzyme should efficiently catalyze the oxidative cleavage of a conjugated C=C bond in aromatic olefins to form valuable aromatic aldehydes (Figure 1). Although a previously identified carotenoid

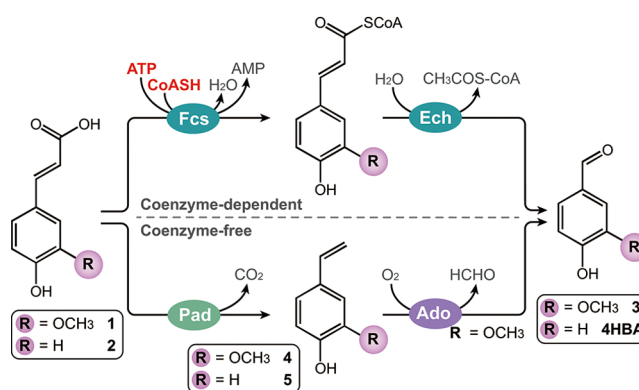


**Figure 1.** Distinct routes for the conversion of **1** and **2**. Fcs and Ech are responsible for the bioconversion of phenolic acids to aromatic aldehydes in a coenzyme-dependent manner. Pad and Ado can convert phenolic acids to aromatic aldehydes in a coenzyme-free fashion. 4HBA = 4-hydroxy benzaldehyde.

oxygenase, Cso2, can transform **4** to **3**, its catalytic efficiency toward **4** is unfortunately extremely low.<sup>15</sup> Moreover, the temperature sensitivity (fairly unstable at 30 °C) and stringent requirement for an alkaline environment severely constrain its industrial application. Therefore, it is vital to identify an efficient and robust Ado to overcome the aforementioned problems.

For preparing the coenzyme-free biocatalyst, we attempted to identify an efficient enzyme for aromatic olefins oxidation without any coenzyme. A BLAST search of the bacterial

Received: August 1, 2018

Published: October 30, 2018

genome sequences revealed the products of *Avi\_5950* from *Agrobacterium vitis* S4, *Hsc\_1401* from *Herbaspirillum seropedicae* AU14040, *Ser39006\_018005* from *Serratia* sp. ATCC 39006, and *Pfluolipicf7\_18165* from *Pseudomonas fluorescens* P1CF7 with significant amino acid identities (57–67%) to Cso2 (Figure S1), and they were promising candidates for the oxidation of **4**. However, regrettably, **3** could not be detected from whole cells expressing these genes by feeding **4**. As the search scope was expanded, a thermophilic fungus, *Thermothelomyces thermophila*, attracted our attention.<sup>21,22</sup> The whole cells of *E. coli* harboring a hypothetical protein (XP\_003665585) from *T. thermophila* successfully converted **4** to **3** (Figure 2A). The presumed Ado with a

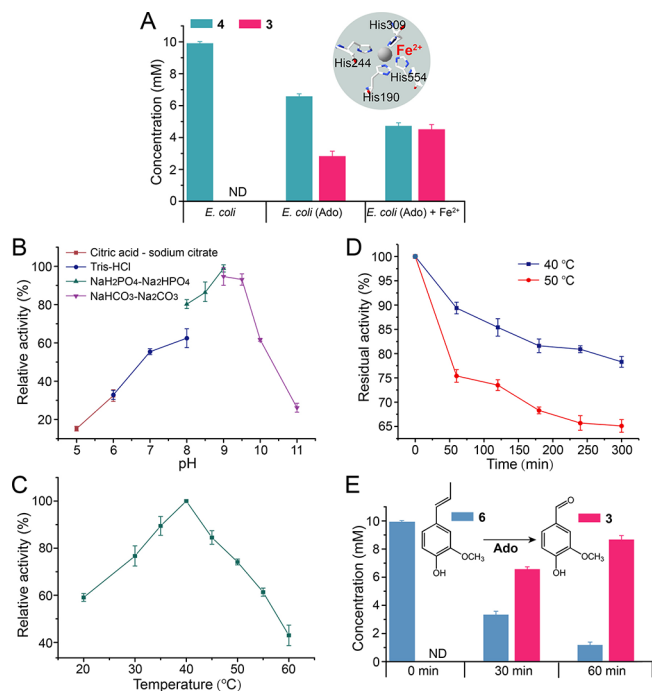


**Figure 2.** Activity assay of the Ado. (A) Biotransformation of **4** to **3** by whole cells. Effects of pH (B) and temperature (C) on Ado activity. (D) Thermal stability of Ado. (E) Biotransformation of **6** to **3** by purified Ado.

theoretical molecular weight of 67.3 kDa shares only 44% amino acid identity with Cso2, and the relationship of Ado with other oxygenases is shown in Figure S2. Normally, the carotenoid oxygenase family contains an Fe<sup>2+</sup>-4-His arrangement as a prosthetic group.<sup>23,24</sup> The four histidines (His<sup>167</sup>, His<sup>218</sup>, His<sup>283</sup>, and His<sup>480</sup>) in Ado might be responsible for combining Fe<sup>2+</sup>. The addition of FeCl<sub>2</sub> improved the activity of the whole cells expressing Ado by 1.6-fold, implying that Ado is a Fe<sup>2+</sup>-containing protein (Figure 2A). Subsequently, Ado was purified, and the molecular mass of purified enzyme was in accordance with the expected value (Figure S3).

The purified Ado was further characterized in terms of its enzymatic properties (Figure 2). The optimum temperature for activity of Ado was 40 °C, and the enzyme presented over 60% of the relative activity even at 55 °C (Figure 2B). Moreover, the Ado was relatively stable at 40 and 50 °C, and more than 60% of the initial activity residue was detected after 300 min of incubation (Figure 2C). The optimum pH of Ado was pH 7.0, and over 60% of the relative activity was detected over a pH range of 7.0 to 10.0 (Figure 2D). The  $K_m$  and  $V_{max}$

values of Ado were determined as 2.7 mM and 0.037 mM/min, respectively, for **4** (Figure S4). The catalytic efficiency ( $k_{cat}/K_m$ ) value was 1.2 mM<sup>-1</sup> s<sup>-1</sup>, which was more than 78 500-fold higher than that of Cso2.<sup>15</sup> Furthermore, Ado shared moderate amino acid identity (34%) with the isoeugenol monooxygenase from *P. nitroreducens* Jin1, which lost all activity by incubation at 50 °C.<sup>25</sup> We speculated that Ado may also possess the ability to convert isoeugenol (**6**), another lignin-related renewable source,<sup>26</sup> to **3** (Figure 2E). This was indeed the case, and the  $K_m$  and  $V_{max}$  values of Ado for **6** were 2.0 mM and 0.060 mM/min, respectively (Figure S5). The catalytic efficiency value was 2.6 mM<sup>-1</sup> s<sup>-1</sup>. The remarkable catalytic efficiency and good thermal stability make Ado an ideal candidate for coenzyme-free biocatalysis.

Previously, we found that high temperature can deactivate the redundant endogenous alcohol dehydrogenases (ADHs) in the whole-cell biocatalyst for accumulation of aromatic aldehydes.<sup>27</sup> Although the Pad that catalyzes the nonoxidative decarboxylation of **1** has been well studied,<sup>17,18</sup> a Pad with high temperature tolerance is necessary to construct a coenzyme-free biocatalyst. *Bacillus coagulans* DSM1, a thermophilic bacterium that can degrade **1**, contains a putative phenolic acid decarboxylase (BcPad) that shares 79% amino acid identity with Pad from *B. subtilis* (Figure S6). Enzymes from thermophilic bacteria might be more stable, and thus, BcPad was purified and characterized (Figure S7). The optimum pH of BcPad was pH 6.0, and over 70% of the relative activity was detected in a pH range of 5.0 to 7.0 (Figure 3A). The optimum

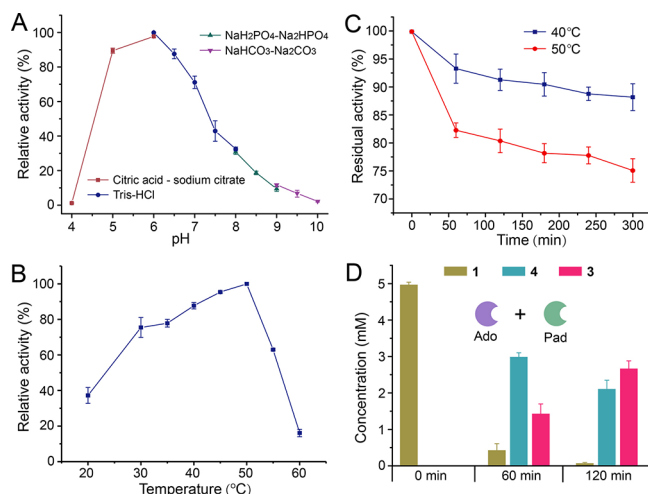


**Figure 3.** Activity assay of the BcPad. Effects of pH (A) and temperature (B) on BcPad activity. (C) Thermal stability of BcPad. (D) Biotransformation of **1** to **3** by BcPad and Ado cocktail.

temperature of BcPad was 50 °C, and the enzyme retained over 60% of its relative activity even at 55 °C (Figure 3B). Moreover, BcPad was relatively stable at 40 and 50 °C (Figure 3C). The  $K_m$  and  $V_{max}$  values of BcPad for **1** were determined as 1.9 mM and 1.087 mM/min, respectively, whereas those of BcPad for **2** were 3.6 mM and 3.395 mM/min (Figure S8), respectively. BcPad showed an 801-fold and 240-fold higher  $k_{cat}/K_m$  value (58.4 mM<sup>-1</sup> s<sup>-1</sup>) for **2** compared to those of Pads from *B. subtilis* and *Lactobacillus plantarum*.<sup>28</sup> Subsequently, one-pot multistep synthesis of **3** without any coenzyme was carried out using purified the BcPad and Ado cocktail (Figure 3D), which implies that BcPad was an ideal constituent for use in conjunction with Ado.

The coenzyme-free biocatalyst LV (Lignin-to-Valuables) was constructed by coexpression of the aforementioned BcPad and Ado (Figure S9A). After reaction for 2 h with LV at 30 °C, 30.0 mM of **1** was converted into 7.1 mM of **3**, and 9.7 mM vanillyl alcohol (**7**) was also formed due to the activities of endogenous ADHs (Figure 4). When the reaction temperature

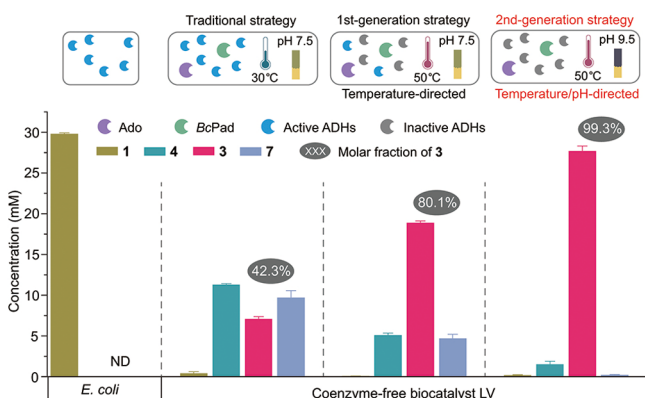


**Figure 4.** Temperature/pH-directed formation of **3** by biocatalyst LV. **1** was converted to **3** and **7** at 30 °C and pH 7.5. When the temperature and pH value were increased to 50 °C and pH 9.5, **1** was mainly converted into **3**.

was increased to 50 °C, the same amount of **1** was converted into 18.9 mM of **3**. Although this temperature-directed strategy partially deactivates the redundant ADHs,<sup>27</sup> 4.7 mM of **3** was still converted to **7** (Figure 4). We propose a second-generation strategy to further deactivate the endogenous ADHs by simultaneously increasing the reaction temperature and pH. As the alkaline environment is more preferred by Ado, the rate-limiting step of the coenzyme-free system, this should be a win–win solution. As expected, 30.0 mM of **1** was mainly converted into 27.7 mM of **3** at 50 °C and pH 9.5, and only 0.2 mM of **7** remained (Figure 4). Thus, the temperature/pH-directed strategy solved the traditional problem of the undesirable activities of endogenous ADHs. The coenzyme-based biocatalyst VA1 was also fed with the same amount of **1**. However, the overwhelming majority of **1** remained (Figure S10). Here, the corresponding productivity of **3** (2.1 g L<sup>-1</sup> h<sup>-1</sup>) by LV far surpasses all previously reported values for whole-cell biocatalysts, which demonstrates the superiority of the coenzyme-free system (Table S1). Moreover, the optimization of stoichiometry based on kinetic models may further improve the efficiency of LV-mediated multienzyme processes.<sup>29–31</sup>

Normally, **2** and **1** are released in a ratio of 1.8:1 after alkaline hydrolysis of many lignin-rich agricultural wastes.<sup>32</sup> Therefore, a mixture of 30 mM of **1** and 54 mM of **2** (1:1.8) was used as substrate to confirm the feasibility of the simultaneous value-added utilization of predominant lignin hydrolytic aromatics. Here, 27.5 mM of **3** and 48.7 mM of **5** were successfully formed in 2 h by the LV-mediated biocatalysis (Figure S9B), and the maximal conversion yields reached 91.7% and 90.2% for **3** and **5**, respectively. A biphasic organic/aqueous system was further used to improve the productivity of the coenzyme-free one-pot reaction. Water-immiscible organic solvents could partly extract the hydrophobic products (i.e., **3** and **5**) from the aqueous phase containing more hydrophilic substrates (i.e., **1** and **2**), thus alleviating the toxic and inhibitory effects of products.<sup>33,34</sup>

Considering the criteria such as equilibrium partition coefficients and product recovery between 22 organic and aqueous phases (Table S2), six solvents were selected (Figure S11). Given the higher reaction yields obtained above, the chloroform/water two-phase system was employed for large-scale production of **3** and **5** using a 1-L bioreactor. LV produced a total of 13.3 g L<sup>-1</sup> of **3** and 20.5 g L<sup>-1</sup> of **5** within 18 h, as the concentrations of **1** and **2** increased to 100.0 mM and 180.0 mM, respectively (Figure 5). The production of **3** is the highest level achieved to date via biosynthesis using recombinant cells (Table S3).

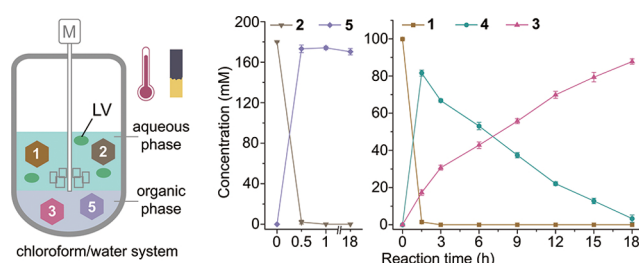


**Figure 5.** Scaled-up production of **3** and **5** using the coenzyme-free biocatalyst LV. A chloroform/water system was employed.

Many other lignin-related aromatics were also investigated as substrates for the coenzyme-free biocatalyst (Figure 6). Besides

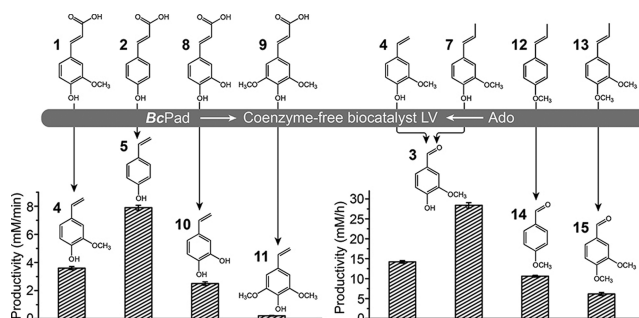


**Figure 6.** Productivity of various valuable aromatics with coenzyme-free biocatalyst LV. Besides **1**, **2**, **4**, and **6**, LV catalyzes other lignin-derived aromatics, **8**, **9**, **12**, and **13**, to form **10**, **11**, **14**, and **15**, respectively.

**4** and **6**, LV catalyzes the nonoxidative decarboxylation of caffeic acid (**8**) and sinapic acid (**9**), resulting in the formation of 3,4-dihydroxystyrene (**10**) and 4-hydroxy-3,5-dimethoxystyrene (**11**), respectively. **10** and **11** are important aromatic monomers for the production of high-performance polymers.<sup>35,36</sup> Moreover, the biocatalyst LV catalyzes the oxidative cleavage of anethole (**12**) and *O*-methyl isoeugenol (**13**) to form anisaldehyde (**14**) and veratraldehyde (**15**), respectively, which are valuable materials with applications in perfumery, agrochemical, and pharmaceutical industries.<sup>29,37</sup> Thus, this coenzyme-free biocatalyst provides a green route for the value-added utilization of numerous lignin-derived aromatics.

In summary, a useful aromatic phenol monooxygenase was identified and characterized here. Coupled with a phenolic acid decarboxylase, the coenzyme-free biocatalyst LV was constructed for value-added utilization of lignin-derived aromatics. LV showed outstanding catalytic performance in biphasic organic/aqueous systems and efficiently converted the predominant aromatic monomers of lignin into valuable

aromatics without the need for any expensive coenzyme. Moreover, the versatile coenzyme-free biocatalyst may be extended to generate a variety of valuable chemicals from other renewable lignin-related aromatics. The temperature/pH-directed catalytic strategy described herein can be used for the biosynthesis of other valuable aldehydes used in industrial applications. This green route for converting lignin to value-added products can facilitate the comprehensive use of agricultural wastes and enhance the entire efficiency of biorefineries.

## ■ ASSOCIATED CONTENT

### Supporting Information

The Supporting Information is available free of charge on the ACS Publications website at DOI: 10.1021/jacs.8b08177.

Materials and methods, Figures S1 to S11 and Tables S1 to S5 (PDF)

## ■ AUTHOR INFORMATION

### Corresponding Author

\*pingxu@sytu.edu.cn

### ORCID

Ping Xu: 0000-0002-4418-9680

### Notes

The authors declare no competing financial interest.

## ■ ACKNOWLEDGMENTS

We acknowledge the financial support from the China Postdoctoral Science Foundation (2017M611547 and 2018T110391). The authors are thankful for partial financial support by the Science and Technology Commission of Shanghai Municipality (17JC1404800) and for grants from the National Natural Science Foundation of China (31800019 and 21777098).

## ■ REFERENCES

- (1) De Bruyn, M.; Fan, J.; Budarin, V. L.; Macquarrie, D. J.; Gomez, L. D.; Simister, R.; Farmer, M. T. J.; Raverty, W. D.; McQueen-Mason, S. J.; Clark, J. H. A new perspective in bio-refining: levoglucosone and cleaner lignin from waste biorefinery hydrolysis lignin by selective conversion of residual saccharides. *Energy Environ. Sci.* **2016**, *9*, 2571–2574.
- (2) Wang, C.; Wang, L.; Zhang, J.; Wang, H.; Lewis, J. P.; Xiao, F. S. Product selectivity controlled by zeolite crystals in biomass hydrogenation over a palladium catalyst. *J. Am. Chem. Soc.* **2016**, *138*, 7880–7883.
- (3) Alonso, D. M.; Hakim, S. H.; Zhou, S.; Won, W.; Hosseinaei, O.; Tao, J.; Garcia-Negron, V.; Motagamwala, A. H.; Mellmer, M. A.; Huang, K.; Houtman, C. J.; Labbé, N.; Harper, D. P.; Maravelias, C. T.; Runge, T.; Dumesic, J. A. Increasing the revenue from lignocellulosic biomass: Maximizing feedstock utilization. *Sci. Adv.* **2017**, *3*, e1603301.
- (4) Wu, W.; Liu, F.; Singh, S. Toward engineering *E. coli* with an autoregulatory system for lignin valorization. *Proc. Natl. Acad. Sci. U. S. A.* **2018**, *115*, 2970–2975.
- (5) Renders, T.; Van den Bosch, S.; Koelewijn, S. F.; Schutyser, W.; Sels, B. F. Lignin-first biomass fractionation: the advent of active stabilisation strategies. *Energy Environ. Sci.* **2017**, *10*, 1551–1557.
- (6) Wang, M.; Liu, M.; Li, H.; Zhao, Z.; Zhang, X.; Wang, F. Carbon modification of nickel catalyst for depolymerization of oxidized lignin to aromatics. *ACS Catal.* **2018**, *8*, 1614–1620.
- (7) Lahive, C. W.; Deuss, P. J.; Lancefield, C. S.; Sun, Z.; Cordes, D. B.; Young, C. M.; Tran, F.; Slawin, A. M. Z.; de Vries, J. D.; Kamer, P. C. J.; Westwood, N. J.; Barta, K. Advanced model compounds for

understanding acid-catalyzed lignin depolymerization: Identification of renewable aromatics and a lignin-derived solvent. *J. Am. Chem. Soc.* **2016**, *138*, 8900–8911.

(8) Schutyser, W.; Renders, T.; Van den Bosch, S.; Koelewijn, S. F.; Beckham, G. T.; Sels, B. F. Chemicals from lignin: an interplay of lignocellulose fractionation, depolymerisation, and upgrading. *Chem. Soc. Rev.* **2018**, *47*, 852–908.

(9) Shuai, L.; Amiri, M. T.; Questell-Santiago, Y. M.; Héroguel, F.; Li, Y.; Kim, H.; Meilan, R.; Chapple, C.; Ralph, J.; Luterbacher, J. S. Formaldehyde stabilization facilitates lignin monomer production during biomass depolymerization. *Science* **2016**, *354*, 329–333.

(10) Luterbacher, J. S.; Azarpira, A.; Motagamwala, A. H.; Lu, F.; Ralph, J.; Dumesic, J. A. Lignin monomer production integrated into the  $\gamma$ -valerolactone sugar platform. *Energy Environ. Sci.* **2015**, *8*, 2657–2663.

(11) Rinaldi, R.; Jastrzebski, R.; Clough, M. T.; Ralph, J.; Kennema, M.; Bruijninx, P. C.; Weckhuysen, B. M. Paving the way for lignin valorisation: recent advances in bioengineering, biorefining and catalysis. *Angew. Chem., Int. Ed.* **2016**, *55*, 8164–8215.

(12) Kristufek, S. L.; Wacker, K. T.; Tsao, Y. Y. T.; Su, L.; Wooley, K. L. Monomer design strategies to create natural product-based polymer materials. *Nat. Prod. Rep.* **2017**, *34*, 433–459.

(13) Kunjapur, A. M.; Tarasova, Y.; Prather, K. L. Synthesis and accumulation of aromatic aldehydes in an engineered strain of *Escherichia coli*. *J. Am. Chem. Soc.* **2014**, *136*, 11644–11654.

(14) Ni, J.; Tao, F.; Du, H.; Xu, P. Mimicking a natural pathway for de novo biosynthesis: natural vanillin production from accessible carbon sources. *Sci. Rep.* **2015**, *5*, 13670.

(15) Furuya, T.; Miura, M.; Kino, K. A coenzyme-independent decarboxylase/oxygenase cascade for the efficient synthesis of vanillin. *ChemBioChem* **2014**, *15*, 2248–2254.

(16) Wang, J.; Mahajani, M.; Jackson, S. L.; Yang, Y.; Chen, M.; Ferreira, E. M.; Lin, Y.; Yan, Y. Engineering a bacterial platform for total biosynthesis of caffeic acid derived phenethyl esters and amides. *Metab. Eng.* **2017**, *44*, 89–99.

(17) Himo, F. Recent trends in quantum chemical modeling of enzymatic reactions. *J. Am. Chem. Soc.* **2017**, *139*, 6780–6786.

(18) Sheng, X.; Himo, F. Theoretical study of enzyme promiscuity: mechanisms of hydration and carboxylation activities of phenolic acid decarboxylase. *ACS Catal.* **2017**, *7*, 1733–1741.

(19) Kang, D. H.; Choi, W. Y.; Woo, H.; Jang, S.; Park, H. Y.; Shim, J.; Choi, J. W.; Kim, S.; Jeon, S.; Lee, S.; Park, J. H. Poly-4-vinylphenol (PVP) and poly(melamine-co-formaldehyde)(PMF)-based atomic switching device and its application to logic gate circuits with low operating voltage. *ACS Appl. Mater. Interfaces* **2017**, *9*, 27073–27082.

(20) Payer, S. E.; Pollak, H.; Glueck, S. M.; Faber, K. A rational active-site redesign converts a decarboxylase into a C = C hydratase: “tethered acetate” supports enantioselective hydration of 4-hydroxystyrenes. *ACS Catal.* **2018**, *8*, 2438–2442.

(21) Fürst, M. J.; Savino, S.; Dudek, H. M.; Gómez Castellanos, J. R.; Gutiérrez de Souza, C.; Rovida, S.; Fraaije, M. W.; Mattevi, A. Polycyclic ketone monooxygenase from the thermophilic fungus *Thermothelomyces thermophila*: A structurally distinct biocatalyst for bulky substrates. *J. Am. Chem. Soc.* **2017**, *139*, 627–630.

(22) Singh, B. *Myceliophthora thermophila* syn. *Sporotrichum thermophile*: a thermophilic mould of biotechnological potential. *Crit. Rev. Biotechnol.* **2016**, *36*, 59–69.

(23) Kiser, P. D. Reappraisal of dioxygen binding in NOVI crystal structures. *Proc. Natl. Acad. Sci. U. S. A.* **2017**, *114*, 6027–6028.

(24) McAndrew, R. P.; Sathitsuksanoh, N.; Mbughuni, M. M.; Heins, R. A.; Pereira, J. H.; George, A.; Sale, K. L.; Fox, B. G.; Simmons, B. A.; Adams, P. D. Structure and mechanism of NOVI, a resveratrol-cleaving dioxygenase. *Proc. Natl. Acad. Sci. U. S. A.* **2016**, *113*, 14324–14329.

(25) Ryu, J. Y.; Seo, J.; Park, S.; Ahn, J. H.; Chong, Y.; Sadowsky, M. J.; Hur, H. G. Characterization of an isoeugenol monooxygenase (Iem) from *Pseudomonas nitroreducens* Jin1 that transforms isoeugenol to vanillin. *Biosci., Biotechnol., Biochem.* **2013**, *77*, 289–294.

(26) Marquez-Medina, M. D.; Prinsen, P.; Li, H.; Shih, K.; Romero, A. A.; Luque, R. Continuous-flow synthesis of supported magnetic iron oxide nanoparticles for efficient isoeugenol conversion into vanillin. *ChemSusChem* **2018**, *11*, 389–396.

(27) Ni, J.; Gao, Y. Y.; Tao, F.; Liu, H. Y.; Xu, P. Temperature-directed biocatalysis for the sustainable production of aromatic aldehydes or alcohols. *Angew. Chem., Int. Ed.* **2018**, *57*, 1214–1217.

(28) Hu, H.; Li, L.; Ding, S. An organic solvent-tolerant phenolic acid decarboxylase from *Bacillus licheniformis* for the efficient bioconversion of hydroxycinnamic acids to vinyl phenol derivatives. *Appl. Microbiol. Biotechnol.* **2015**, *99*, 5071–5081.

(29) Riemer, D.; Mandaviya, B.; Schilling, W.; Götz, A. C.; Kühl, T.; Finger, M.; Das, S. CO<sub>2</sub>-catalyzed oxidation of benzylic and allylic alcohols with DMSO. *ACS Catal.* **2018**, *8*, 3030–3034.

(30) Thomas, A. A.; Wang, H.; Zahrt, A. F.; Denmark, S. E. Structural, kinetic, and computational characterization of the elusive arylpalladium (II) boronate complexes in the Suzuki–Miyaura reaction. *J. Am. Chem. Soc.* **2017**, *139*, 3805–3821.

(31) Chado, G. R.; Stoykovich, M. P.; Kaar, J. L. Role of dimension and spatial arrangement on the activity of biocatalytic cascade reactions on scaffolds. *ACS Catal.* **2016**, *6*, 5161–5169.

(32) Linh, T. N.; Fujita, H.; Sakoda, A. Release kinetics of esterified *p*-coumaric acid and ferulic acid from rice straw in mild alkaline solution. *Bioresour. Technol.* **2017**, *232*, 192–203.

(33) Rudroff, F.; Mihovilovic, M. D.; Gröger, H.; Snajdrova, R.; Iding, H.; Bornscheuer, U. T. Opportunities and challenges for combining chemo- and biocatalysis. *Nat. Catal.* **2018**, *1*, 12–22.

(34) Zhang, M.; Wei, L.; Chen, H.; Du, Z.; Binks, B. P.; Yang, H. Compartmentalized droplets for continuous flow liquid–liquid interface catalysis. *J. Am. Chem. Soc.* **2016**, *138*, 10173–10183.

(35) North, M. A.; Del Grosso, C. A.; Wilker, J. J. High strength underwater bonding with polymer mimics of mussel adhesive proteins. *ACS Appl. Mater. Interfaces* **2017**, *9*, 7866–7872.

(36) Payra, D.; Fujii, Y.; Das, S.; Takaishi, J.; Naito, M. Rational design of a biomimetic glue with tunable strength and ductility. *Polym. Chem.* **2017**, *8*, 1654–1663.

(37) Matsuoka, J.; Matsuda, Y.; Kawada, Y.; Oishi, S.; Ohno, H. Total synthesis of dictyodendrins by the gold-catalyzed cascade cyclization of conjugated diynes with pyrroles. *Angew. Chem.* **2017**, *129*, 7552–7556.

#### ■ NOTE ADDED AFTER ASAP PUBLICATION

Figures 2 and 3 and the Figure 1 caption were corrected on November 6, 2018.